Available online at www.sciencedirect.com
ScienceDirect
Bioorganic & Medicinal Chemistry Letters 18 (2008) 2250–2255
Bioorganic & Medicinal Chemistry Letters

Discovery of novel PRL-3 inhibitors based on the structure-based virtual screening

Hwangseo Park,[a,*] Suk-Kyeong Jung,[b] Dae Gwin Jeong,[c] Seong Eon Ryu[c] and Seung Jun Kim[b,*]

[a]*Department of Bioscience and Biotechnology, Sejong University, 98 Kunja-Dong, Kwangjin-Ku, Seoul 143-747, Republic of Korea*
[b]*Translational Research Center, Korea Research Institute of Bioscience and Biotechnology, 52 Eoeun-Dong, Yuseong-Gu, Daejeon 305-333, Republic of Korea*
[c]*Systemic Proteomics Research Center, Korea Research Institute of Bioscience and Biotechnology, 52 Eoeun-Dong, Yuseong-Gu, Daejeon 305-333, Republic of Korea*

Received 19 November 2007; revised 14 February 2008; accepted 6 March 2008
Available online 10 March 2008

Abstract—The inhibitors of phosphatase of regenerating liver-3 (PRL-3) have been shown to be useful as therapeutics for the treatment of cancer. We have been able to identify 12 novel PRL-3 inhibitors by means of the virtual screening with docking simulations under the consideration of the effects of ligand solvation in the scoring function. Because the newly identified inhibitors are structurally diverse and reveal a significant potency with IC_{50} values ranging from 10 to 50 μM, all of them can be considered for further development by structure–activity relationship or de novo design methods. Structural features relevant to the interactions of the newly identified inhibitors with the amino acid residues in the active site and the peripheral binding site of PRL-3 are discussed in detail.

Protein tyrosine phosphatases (PTPs) are a family of closely related key regulatory enzymes that dephosphorylate phosphotyrosine residues in their protein substrates. So far much evidence has been reported in support of the correlation between malfunctions in PTP activity and various diseases including cancer, neurological disorders, and diabetes.[1] This has made PTPs be a promising target for therapeutic intervention. Among a variety of PTPs, the phosphatase of regenerating liver (PRL) family tyrosine phosphatases (PRL-1, PRL-2, and PRL-3) are closely related intracellular enzymes and possess the PTP active-site signature sequence of CX_5R.[2,3] They share at least 75% of amino acids and are similar in size with molecular weight of about 20 kDa.

PRL-3 is a nonclassical PTP with C-terminal prenylation motif and is recently known to be related with metastasis. It resides at the nucleus and the cytoplasmic membrane in the nonprenylated and prenylated states, respectively. Overexpression of PRL-3 has proven to cause the transformation of human embryonic kidney cell HEK293 as well as the increase in HEK293 cell growth.[4] A consistent increase in the expression of PRL-3 mRNA in the liver metastasis of colorectal cancers provided evidence for the correlation between the overexpression of PRL-3 with colorectal cancer metastasis.[5] Furthermore, it was shown that the cell motility, invasion activity, and metastasis were promoted with the increase in the catalytic activity of PRL-3.[6] Thus, a series of experimental evidence indicates that PRL-3 can serve as a therapeutic target for metastatic tumors as well as a putative prognostic marker.

The structural studies have shown that PRL phosphatases belong to a class of dual specificity phosphatases with the closest structural homology to VHR phosphatases. The characteristic structural features that discriminate PRL-3 from the other phosphatases include the unusually hydrophobic active site without the catalytically important serine/threonine residue.[7] The nuclear magnetic resonance (NMR) data for the conformational

Keywords: Virtual screening; Docking; PRL-3; Inhibitor; Anti-cancer agents.
* Corresponding authors. Tel.: +82 2 3408 3766; fax: +82 2 3408 3334 (H.P.), tel.: +82 42 860 4242; fax: +82 42 860 4598 (S.J.K.); e-mail addresses: hspark@sejong.ac.kr; ksj@kribb.re.kr

0960-894X/$ - see front matter © 2008 Elsevier Ltd. All rights reserved.
doi:10.1016/j.bmcl.2008.03.013

motion of PRL-3 indicated an extraordinarily high flexibility of the loop structure comprising the active site. However, such a high-amplitude motion of the flexible loop is damped out upon binding of a substrate analogue.[8] The structure of PRL-1 is similar to that of PRL-3 in that it has a shallow active site pocket with highly hydrophobic character as shown in the X-ray crystal structures, which is not surprising for a high sequence identity of more than 75% between the PRL phosphatases.[9,10] However, molecular modeling studies indicated that each PRL phosphatase would have a unique surface element that can be important for specificity in the catalysis.[7]

Discovery of PRL phosphatase inhibitors has lagged behind the pharmacological and structural studies. Only two classes of inhibitors have been reported so far. Pentamidine proved to be an effective inhibitor of PRL phosphatases with anti-cancer potential.[11] Recently, Ahn et al. identified the rhodanine skeleton in the course of the search for PRL-3 inhibitors through high throughput screening (HTS) of a chemical library.[12] They also reported the synthetic methods and the structure–activity relationship (SAR) data for various rhodanine derivatives as PRL-3 inhibitors.

In the present study, we identify the novel classes of PRL-3 inhibitors by means of a structure-based drug design protocol involving the virtual screening with docking simulations and in vitro enzyme assay. The characteristic feature that discriminates our virtual screening approach from the others lies in the implementation of an accurate solvation model in calculating the binding free energy between PRL-3 and putative ligands, which would have an effect of increasing the hit rate in enzyme assay.[13,14] To the best of our knowledge, we report the first example for the successful application of the structure-based virtual screening to identify novel PRL-3 inhibitors. It will be shown that the docking simulation with the improved binding free energy function can be a useful tool for elucidating the activities of the identified inhibitors, as well as for enriching the chemical library used in screening assays with molecules that are likely to have biological activities.

Although two NMR structures of PRL-3 have been reported in the ligand-free forms,[7,8] they are inappropriate to be used in docking simulation of putative inhibitors because the active site region is maintained flat and exposed to bulk solvent. In order to obtain another conformation of PRL-3 suitable for structure-based virtual screening, therefore, we carried out the homology modeling using the X-ray crystal structure of PRL-1 (PDB ID: 1xm2)[10] as the structural template. Due to a high sequence identity of more than 75% between the two PRL phosphatases, a high-quality 3-D structure of PRL-3 is expected in the homology modeling.[15] A special attention was paid to assign the protonation states of the ionizable Asp, Glu, His, and Lys residues of the homology-modeled PRL-3 structure. The side chains of Asp and Glu residues were assumed to be neutral if one of their carboxylate oxygens pointed toward a hydrogen-bond accepting group including the backbone aminocarbonyl oxygen at a distance within 3.5 Å, a generally accepted distance limit for a hydrogen bond of moderate strength.[16] Similarly, the lysine side chains were assumed to be protonated unless the NZ atom was in proximity of a hydrogen bond donating group. The same procedure was also applied to determine the protonation states of ND and NE atoms in His residues.

The docking library for PRL-3 comprising about 85,000 compounds was constructed from the latest version of the chemical database distributed by Interbioscreen (http://www.ibscreen.com) containing approximately 30,000 natural and 320,000 synthetic compounds. The selection was based on the drug-like filters that adopt only the compounds with physicochemical properties of potential drug candidates[17] and without reactive functional group(s). All of the compounds included in the docking library were then subjected to the Corina program to generate their 3-D atomic coordinates, followed by the assignment of Gasteiger–Marsilli atomic charges.[18] We used the AutoDock program[19] in the virtual screening of PRL-3 inhibitors because the outperformance of its scoring function over those of the others had been shown in several target proteins.[20] AMBER force field parameters were assigned for calculating the van der Waals interactions and the internal energy of a ligand as implemented in the AutoDock program. Docking simulations with AutoDock were then carried out in the active site of PRL-3 to score and rank the compounds in the docking library according to their calculated binding affinities.

In the actual docking simulation of the compounds in the docking library, we used the empirical AutoDock scoring function improved by the implementation of a new solvation model for a compound. The modified scoring function has the following form:

$$\begin{aligned}\Delta G^{\mathrm{aq}}_{\mathrm{bind}} = {} & W_{\mathrm{vdW}} \sum_{i=1} \sum_{j>i} \left(\frac{A_{ij}}{r_{ij}^{12}} - \frac{B_{ij}}{r_{ij}^{6}} \right) \\ & + W_{\mathrm{hbond}} \sum_{i=1} \sum_{j>i} E(t) \left(\frac{C_{ij}}{r_{ij}^{12}} - \frac{D_{ij}}{r_{ij}^{10}} \right) \\ & + W_{\mathrm{elec}} \sum_{i=1} \sum_{j>i} \frac{q_i q_j}{\varepsilon(r_{ij}) r_{ij}} + W_{\mathrm{tor}} N_{\mathrm{tor}} \\ & + W_{\mathrm{sol}} \sum_{i=1} S_i \left(\mathrm{Occ}_i^{\max} - \sum_{j>i} V_j \mathrm{e}^{-\frac{r_{ij}^2}{2\sigma^2}} \right), \end{aligned} \tag{1}$$

where W_{vdW}, W_{hbond}, W_{elec}, W_{tor}, and W_{sol} are the weighting factors of van der Waals, hydrogen bond, electrostatic interactions, torsional term, and desolvation energy of inhibitors, respectively. r_{ij} represents the interatomic distance, and A_{ij}, B_{ij}, C_{ij}, and D_{ij} are related to the depths of the potential energy well and the equilibrium separations between the two atoms. The hydrogen bond term has an additional weighting factor, $E(t)$, representing the angle-dependent directionality. With respect to the distance-dependent dielectric constant, $\varepsilon(r_{ij})$, a sigmoidal function proposed by Mehler and Solmajer[21] was used in computing the interatomic elec-

trostatic interactions between PRL-3 and a putative ligand. In the entropic term, N_{tor} is the number of sp^3 bonds in the ligand. In the desolvation term, S_i and V_i are the solvation parameter and the fragmental volume of atom i,[22] respectively, while Occ_i^{max} stands for the maximum atomic occupancy. In the calculation of molecular solvation free energy term in Eq. 1, we used the atomic parameters recently developed by Kang et al.[23] because those of the atoms other than carbon were unavailable in the current version of AutoDock. This modification of the solvation free energy term is expected to increase the accuracy in virtual screening because the underestimation of ligand solvation often leads to the overestimation of the binding affinity of a ligand with many polar atoms.[14]

Of the 85,000 compounds subject to the virtual screening with docking simulations, 200 top-scored compounds were selected as virtual hits. One hundred and ninety-one of them were available from the compound supplier and were evaluated for in vitro inhibitory activity against recombinant human PRL-3. PRL-3 protein was overexpressed using *Escherichia coli* BL21(DE3) strain and subsequently purified. Assays were performed by monitoring the hydrolysis of 6,8-difluoro-4-methylumbelliferyl phosphate (DIFMUP) at 25 °C for 5 min in 20 mM Tris–HCl (pH 8.0), 5 mM DTT, in the presence or absence of the inhibitor. After the addition of purified PRL-3 (0.3 μM) and DIFMUP (5 μM), the reaction mixture was incubated for 5 min. The reaction was stopped by the addition of sodium orthovanadate (20 mM). The phosphatase activities were measured by the absorbance changes caused by the hydrolysis of the substrate at 460 nm. IC_{50} values were an average of triplicate experiments as determined from direct regression curve analysis. Pentamidine was used as a reference.

As a result of in vitro enzyme inhibition assay, we identified 38 compounds that inhibited the catalytic activity of PRL-3 by more than 50% at the concentration of 50 μM. Among them, 12 compounds shown in Figure 1 revealed a high potency with more than 70% inhibition at the same concentration and were selected to determine IC_{50} values. The chemical structures and the inhibitory activities of the newly identified inhibitors are shown in Figure 1 and Table 1, respectively. We note that compound **1** belongs to the rhodanine derivatives that were known as PRL-3 inhibitors in the previous study.[12] This consistency supports the reliability of the virtual screening employed in this work. To the best of our knowledge, the other compounds shown in Figure 1 have not been reported as PRL-3 inhibitors so far. Furthermore, the newly found inhibitors are structurally diverse, and therefore each of which can be considered as a new inhibitor scaffold for further development by structure–activity relationship (SAR) or de novo design methods.

To obtain some energetic and structural insight into the inhibitory mechanisms by the identified inhibitors of

Table 1. IC_{50} values (in μM) of the reference and compounds **1**–**12** against PRL-3 together with their rankings in virtual screening

Compound	IC_{50} (μM)	Ranking	Compound	IC_{50} (μM)	Ranking
Pentamidine	53.6		**7**	44.7	195
1	13.3	23	**8**	37.8	51
2	28.1	8	**9**	27.7	36
3	40.3	189	**10**	41.7	151
4	41.5	54	**11**	18.3	43
5	15.4	94	**12**	48.7	115
6	43.8	22			

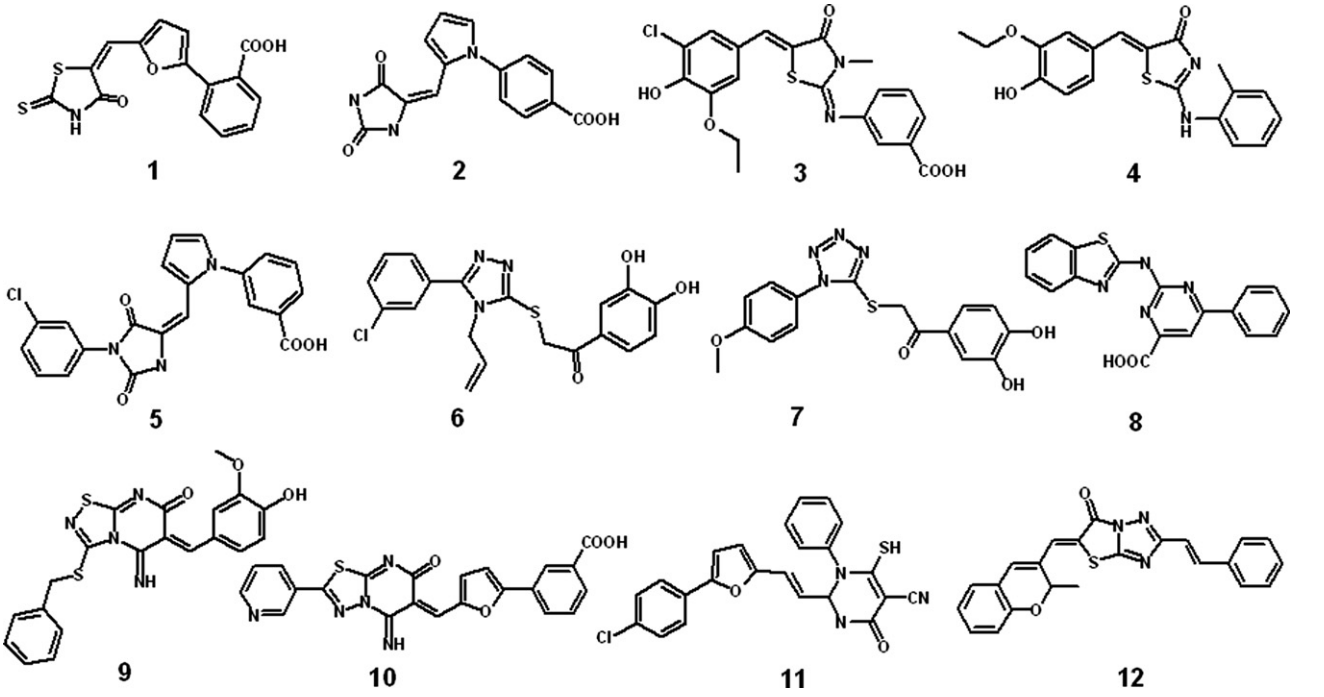

Figure 1. Chemical structures of the newly identified PRL-3 inhibitors.

PRL-3, their binding modes around the active site were investigated using the AutoDock program with the procedure described above. The calculated binding mode of **1** around the active site of PRL-3 is shown in Figure 2. It is noted that the carboxylate group of the inhibitor receives two hydrogen bonds from the backbone amidic nitrogen of Val105 and the side chain of Arg110. Because these two hydrogen bonds are established in the vicinity of the catalytic residue Cys104, the benzoate moiety seems to be an effective chemical group for binding in the active site of PRL-3 and thereby for inhibiting its catalytic activity. A stable hydrogen bond is also established between the aminocarbonyl oxygen of the inhibitor and the backbone amidic nitrogen Gly73. This interaction should also be important in the inhibition of PRL-3 because Gly73 is one of the loop residues comprising the active site and known to be involved in binding of a substrate analogue.[8] Inhibitor **1** can be further stabilized by the hydrophobic interactions of the rhodanine moiety with the side chains of Pro75, Val113, and Tyr148. The inhibitor rhodanine group seems thus to be capable of forming a hydrogen bond and van der Waals contacts with the flexible loop (residues 70–80). Therefore, the binding of inhibitor **1** around the active site is expected to decrease the malleability of the flexible loop, which can be an explanation for the observed inhibitory activity. Judging from the overall structural features of the PRL-3-**1** complex derived from docking simulations, the inhibitory activity of **1** is likely to stem from the multiple hydrogen bonds and hydrophobic interactions established simultaneously in the active site.

Figure 3 shows the lowest-energy AutoDock conformation of compound **5** around the active site of PRL-3. The binding mode of **5** differs from that of **1** in that the benzoate group of the inhibitor resides in a hydrophobic pocket including the side chains of Pro75 and Tyr148, and stays distant from the catalytic residue Cys104. In this complex, the inhibitor carboxylate group receives a hydrogen bond from the side chain amide group of Asn142. The role of the surrogate for a substrate phosphate group can be played by the imidazolidine-2,4-dione moiety of **5**, because one of the aminocarbonyl oxygens forms a hydrogen bond with

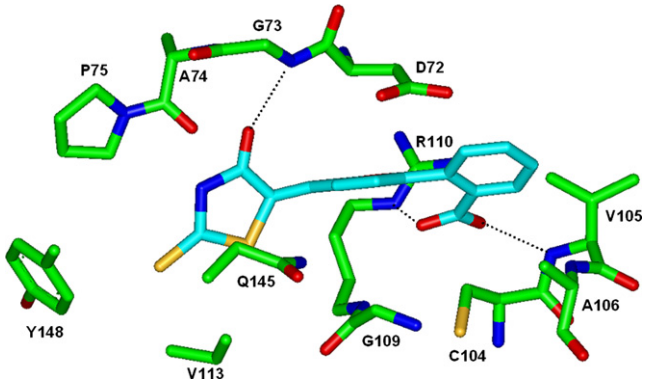

Figure 2. Binding mode of **1** around the active site of PRL-3. Carbon atoms of the protein and the ligand are indicated in green and cyan, respectively. Each dotted line indicates a hydrogen bond.

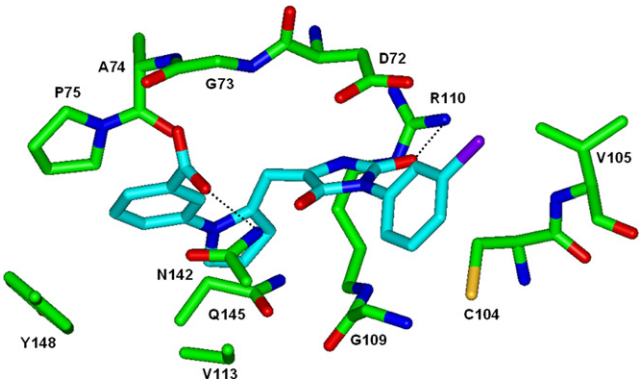

Figure 3. Binding mode of **5** around the active site of PRL-3. Carbon atoms of the protein and the ligand are indicated in green and cyan, respectively. Each dotted line indicates a hydrogen bond.

the side chain of Arg110 that resides in a close proximity to Cys104. However, the number of hydrogen bonds in the enzyme–inhibitor complex decreases from three to two with the change of the inhibitor from **1** to **5**, which would have an effect of lowering the inhibitory activity. Another characteristic feature that discriminates the binding mode of **5** from that of **1** is that the former can be more stabilized in the hydrophobic pocket than the latter. Besides the benzoate group, the pyrrole moiety of **5** also forms a van der Waals contacts with the side chains of Val113, Gln145, and Arg110. Thus, the strengthening of the hydrophobic interactions seems to compensate for the weakening of the hydrogen bond interactions, which can be an explanation for the similarity in inhibitory activities between the two inhibitors.

Although human PTPs have proved to be involved in a variety of diseases, drug discovery with them as a target protein can be hampered due to a close similarity of the active site among PTPs and the resultant difficulty in guaranteeing the selectivity of an inhibitor for a single PTP. In the 3-D structure of PRL-3, a surface cavity separated ~8 Å apart from the active site is found as shown in Figure 4, which is also a structural feature of PRL-1.[9,10] This peripheral binding site comprises the residues from the loop connecting the sheet β4 and the helix α3 (Phe70, Gly73, Ala74, Pro75, and Pro76), those from the helix α4 (Arg110 and Val113), and those from the helix α6 (Lys144, Gln145, and Tyr148). We note that compounds **1** and **5** are accommodated not only in the catalytic site but also in the peripheral binding site of PRL-3, indicating a significant role of the latter in ligand binding. As a check for the presence of such a peripheral binding site in the other PTPs, we searched a surface cavity with the program Voidoo[24] in the 3-D structures of VHR,[25] MKP5,[26] DSP18,[27] VHY,[28] DUSP5,[29] TMDP,[30] and SSH2[31] that are similar in molecular weight to PRL phosphatases. However, the spaces of all the other PTPs corresponding to the surface cavity of PRL-3 were filled with amino acid residues, implying that the presence of a peripheral binding site should be a characteristic feature that discriminates the PRL phosphatases from the other PTPs. The presence of such a peripheral binding site may thus contribute toward the

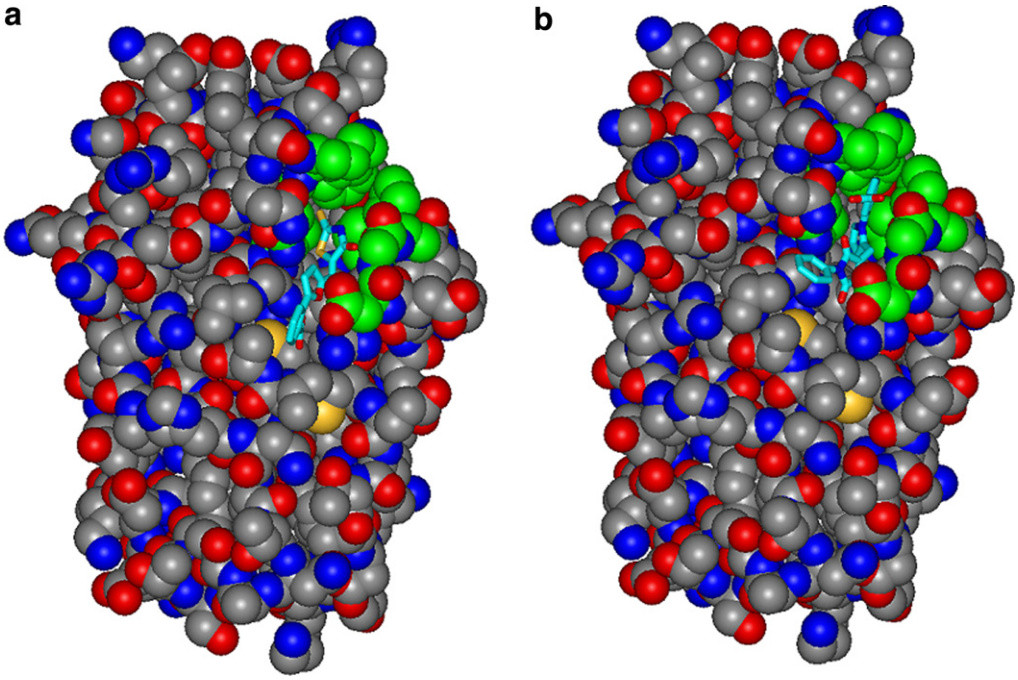

Figure 4. Compounds **1** (a) and **5** (b) bound in the active site and the peripheral binding site of PRL-3. Carbon atoms of the ligand and those forming the peripheral binding site are shown in cyan and green, respectively.

development of a selective PRL phosphatase inhibitor as an anti-cancer drug.

In summary, we have identified 12 new novel inhibitors of PRL-3 by applying a computer-aided drug design protocol involving the homology modeling of the target protein and the structure-based virtual screening with docking simulations under consideration of the effects of ligand solvation in the binding free energy function. These inhibitors reveal a structural diversity as well as a significant potency with IC_{50} values lower than 50 μM. Therefore, each of the newly discovered inhibitors can provide a new scaffold for further development by structure–activity relationship studies or de novo design methods. Detailed binding mode analyses with docking simulation show that the inhibitors can be stabilized by the simultaneous establishment of multiple hydrogen bonds and van der Waals contacts in the active site and the peripheral binding site.

Acknowledgment

This work was supported by the grant from KRIBB Research Initiative Program.

References and notes

1. Waldmann, H.; Bialy, L. *Angew. Chem. Int. Ed.* **2005**, *44*, 3814.
2. Diamone, R. H.; Cressman, D. E.; Laz, T. M.; Abrams, C. S.; Taub, R. *Mol. Cell. Biol.* **1994**, *14*, 3752.
3. Zeng, S.; Bardelli, A.; Buckhaults, P.; Velculescu, V. E.; Rago, C.; St. Croix, B.; Romans, K. E.; Choti, M. A.; Lengauer, C.; Kinzler, K. W.; Vogelstein, B. *Biochem. Biophys. Res. Commun.* **1998**, *244*, 421.
4. Matter, W. F.; Estridge, T.; Zhang, C.; Belagaje, R.; Stancato, L.; Dixon, J.; Johnson, B.; Bloem, L.; Pickard, T.; Donaghue, M.; Acton, S.; Jeyaseelan, R.; Kadambi, V.; Vlahos, C. J. *Biochem. Biophys. Res. Commun.* **2001**, *283*, 1061.
5. Saha, S.; Bardelli, A.; Buckhaults, P.; Velculescu, V. E.; Rago, C.; St. Croix, B.; Romans, K. E.; Choti, M. A.; Lengauer, C.; Kinzler, K. W.; Vogelstein, B. *Science* **2001**, *294*, 1343.
6. Zeng, Q.; Dong, J. M.; Guo, K.; Li, J.; Tan, H. X.; Koh, V.; Pallen, C. J.; Manser, E.; Hong, W. *Cancer Res.* **2003**, *63*, 2716.
7. Kozlov, G.; Cheng, J.; Ziomek, E.; Banville, D.; Gehring, K.; Ekiel, I. *J. Biol. Chem.* **2004**, *279*, 11882.
8. Kim, K. A.; Song, J. S.; Jee, J.; Sheen, M. R.; Lee, C.; Lee, T. G.; Ro, S.; Cho, J. M.; Lee, W.; Yamazaki, T.; Jeon, Y. H.; Cheong, C. *FEBS Lett.* **2004**, *565*, 181.
9. Sun, J. P.; Wang, W. Q.; Yang, H.; Liu, S.; Liang, F.; Fedorov, A. A.; Almo, S. C.; Zhang, Z. Y. *Biochemistry* **2005**, *44*, 12009.
10. Jeong, D. G.; Kim, S. J.; Kim, J. H.; Son, J. H.; Park, M. R.; Lim, S. M.; Yoon, T. S.; Ryu, S. E. *J. Mol. Biol.* **2005**, *345*, 401.
11. Pathak, M. K.; Dhawan, D.; Lindner, D. J.; Borden, E. C.; Farver, C.; Taolin, Y. *Mol. Cancer Ther.* **2002**, *1*, 1255.
12. Ahn, J. H.; Kim, S. J.; Park, W. S.; Cho, S. Y.; Ha, J. D.; Kim, S. S.; Kang, S. K.; Jeong, D. G.; Jung, S.-K.; Lee, S.-H.; Kim, H. M.; Park, S. K.; Lee, K. H.; Lee, C. W.; Ryu, S. E.; Choi, J.-K. *Bioorg. Med. Chem. Lett.* **2006**, *16*, 2996.
13. Zou, X.; Sun, Y.; Kuntz, I. D. *J. Am. Chem. Soc.* **1999**, *121*, 8033.
14. Shoichet, B. K.; Leach, A. R.; Kuntz, I. D. *Proteins* **1999**, *34*, 4.
15. Baker, D.; Sali, A. *Science* **2001**, *294*, 93.
16. Jeffrey, G. A. *An Introduction to Hydrogen Bonding*; Oxford University Press: Oxford, 1997.
17. Lipinski, C. A.; Lombardo, F.; Dominy, B. W.; Feeney, P. J. *Adv. Drug Delivery Rev.* **1997**, *23*, 3.

18. Gasteiger, J.; Marsili, M. *Tetrahedron* **1980**, *36*, 3219.
19. Morris, G. M.; Goodsell, D. S.; Halliday, R. S.; Huey, R.; Hart, W. E.; Belew, R. K.; Olson, A. J. *J. Comput. Chem.* **1998**, *19*, 1639.
20. Park, H.; Lee, J.; Lee, S. *Proteins* **2006**, *65*, 549.
21. Mehler, E. L.; Solmajer, T. *Protein Eng.* **1991**, *4*, 903.
22. Stouten, P. F. W.; Frömmel, C.; Nakamura, H.; Sander, C. *Mol. Simulat.* **1993**, *10*, 97.
23. Kang, H.; Choi, H.; Park, H. *J. Chem. Inf. Model.* **2007**, *47*, 509.
24. Kleywegt, G. J.; Jones, T. A. *Acta Crystallogr. D* **1994**, *50*, 178.
25. Yuvaniyama, J.; Denu, J. M.; Dixon, J. E.; Saper, M. A. *Science* **1996**, *272*, 1328.
26. Jeong, D. G.; Yoon, T.-S.; Kim, J. H.; Shim, M. Y.; Jung, S.-K.; Son, J. H.; Ryu, S. E.; Kim, S. J. *J. Mol. Biol.* **2006**, *360*, 946.
27. Jeong, D. G.; Cho, Y. H.; Yoon, T.-S.; Kim, J. H.; Son, J. H.; Ryu, S. E.; Kim, S. J. *Acta Crystallogr. D* **2006**, *62*, 582.
28. Yoon, T. S.; Jeong, D. G.; Kim, J. H.; Cho, Y. H.; Son, J. H.; Ryu, S. E.; Kim, S. J. *Proteins* **2005**, *61*, 694.
29. Jeong, D. G.; Cho, Y. H.; Yoon, T.-S.; Kim, J. H.; Ryu, S. E.; Kim, S. J. *Proteins* **2007**, *66*, 253.
30. Kim, S. J.; Jeong, D. G.; Yoon, T.-S.; Son, J. H.; Cho, S. K.; Ryu, S. E.; Kim, J.-H. *Proteins* **2007**, *66*, 239.
31. Jung, S.-K.; Jeong, D. G.; Yoon, T.-S.; Kim, J. H.; Ryu, S. E.; Kim, S. J. *Proteins* **2007**, *68*, 408.